This article has been accepted for publication in a future issue of this journal, but has not been fully edited. Content may change prior to final publication. Citation information: DOI 10.1109/TVT.2019.2940460, IEEE Transactions on Vehicular Technology

Analytical Evaluation of Cellular Network Uplink Communications with Higher Order Sectorization Deployments

Jianhua He, Wenyang Guan, Weisi Guo, Wei Liu, and Wenqing Cheng

***Abstract*—Higher Order Sectorization (HOS), which splits macro base stations into a larger number of sectors, is widely considered in the cellular community as a cost-effective means of improving network capacity. We develop two general and low-complexity analytical models to characterize and relate the uplink performance indicators with key dynamic functionalities and variables, such as fractional power control (FPC), directional antenna radiation patterns and the multi-cell inter-cell interference (ICI). The adopted methodology approximates the uplink ICIs from individual cell sectors by log-normal random variables, of which the statistical parameters can be estimated using approaches that trade-off complexity and accuracy. Furthermore, the aggregate uplink ICI is approximated with a log-normal random variable, from which network performance metrics are computed. Compared to two existing baseline analytical methods the proposed analytical models have improved accuracy. The analytical models are applied to evaluate HOS deployments with both regular and irregular cell geometries. Results on sectorization scaling show it is an effective method in capacity scaling, but at the cost of increased outage probability. The proposed theoretical models can be used as a fast and effective tool for performance assessment and optimization of Long-Term Evolution (LTE) and 5G networks.**

***Index terms*—** LTE; Cellular networks; 5G; Higher order sectorization; Uplink communications; Performance modelling

I. Introduction

THE increasing proliferation of affordable smart phones, and the fusion of social-media and multi-media content delivery is driving a strong growth in wireless network traffic. While the baseline Long-Term Evolution (LTE) standards represent a significant capacity improvement, new capacity scaling methods are needed to meet the demands of the future 5G standard [1]–[3]. As a result, emerging system architectures and radio techniques such as small cells, massive and multi-user multiple input multiple output (MIMO), 3D-beamforming, millimeter wave transmission, non-orthogonal multiple access (NOMA) and software defined networks (SDN) have been investigated extensively [1]–[6].

Jianhua He (email: j.he7@aston.ac.uk) is with the School of Engineering and Applied Science, Aston University, UK. Wenyang Guan (email: guanwenyang@btbu.edu.cn) is with School of Computer and Information Engineering, Beijing Technology and Business University, China. Weisi Guo (email: Weisi.Guo@warwick.ac.uk) is with School of Engineering, University of Warwick, UK. Wei Liu (email: liuwei@mail.hust.edu.cn, Corresponding Author) and Wenqing Cheng (email: chengwq@hust.edu.cn) are with the School of Electronic Information and Communications, Huazhong University of Science and Technology, China.

One of the most cost-effective means of improving network capacity has been, and remains to be higher order sectorization (HOS). HOS is cost-efficient by exploiting spatial spectrum reuse without incurring significant capital or operational expenditures, and remains attractive compared to deploying new eNodeBs or frequency carriers [10]–[14]. HOS has been widely evaluated in the cellular community both analytically, numerically, and experimentally [7]–[14]. In the baseline configuration of LTE networks, macrocell eNodeBs are equipped with 3 sectors. Although HOS with 6, 12 or even more sectors per macrocell BS has the potentials of enhancing network capacity, its implementation remains rare. Complementary technologies include adopting MIMO techniques with 12 antennas per site [10]. But compared to the capacity achieving multi-user MIMO technology with 3 antennas per sector, HOS with single antenna transmission per sector produced higher mean site throughput [11]. Throughput and fairness performance of HOS with and without cooperative transmission schemes were analyzed with up to 12 antennas per site [12]. HOS and fractional frequency reuse (FFR) schemes were jointly evaluated by simulation and analysis for orthogonal frequency division multiple access (OFDMA) downlink communication [14]. However, HOS also comes with its own challenges in terms of inter-cell interference (ICI), power control, and mobility management. A fast and effective analytical tool is in high demand for feasibility assessment and optimization of large-scale HOS deployment.

Whilst a great deal of research attention has been given to LTE and 5G networks downlink performance, low complexity computational methods for uplink performance evaluation and optimization remains lacking, especially for HOS. Performance evaluation of cellular wireless networks was more focused on downlink modelling (e.g., [14], [16]–[20]), and somewhat neglected in uplink research [21]–[23]. The complexity of the uplink modelling is greater, as the interference arises from mobile users (as opposed to fixed base stations on the downlink) and more advanced power control schemes are used for uplink communication which further complicates the modelling process [20].

In the literature the existing research studies on modelling cellular network uplink ICI and network performance can be classified into three major categories.

a) Deterministic geometry models: The majority of studies on cellular network uplink communication modeling fall into this category. A widely used model for the uplink ICI is Wyner model [25], in which ICI was assumed to be a

This article has been accepted for publication in a future issue of this journal, but has not been fully edited. Content may change prior to final publication. Citation information: DOI 10.1109/TVT.2019.2940460, IEEE Transactions on Vehicular Technology

weight of aggregate signals transmitted from adjacent cells and the ICI value is left to be determined. It was shown in [26] that the Wyner model is not accurate for cellular networks employing time-division multiple access (TDMA) or OFDMA technologies. Haas and McLaughlin provided a derivation of probability distribution function (PDF) of adjacent channel interference from single cell in the uplink of a cellular system [27]. Similarly Zhu et al. derived PDF of single cell uplink ICI with power control in OFDMA networks [28]. It is noted that aggregate ICI expression is not derived from the PDF of single cell uplink ICI [27] [28], and uplink signal to interference and noise ratio (SINR) and network throughput are not analyzed. Elayoubi *et al.* studied the uplink ICI and capacity in LTE systems without shadowing [29]. Karray studied uplink resource allocation and network performance in both code-division multiple access (CDMA) and OFDMA networks [30]. A framework of modeling uplink ICI was reported with scheduling in [31] and with power compensation schemes in [32]. Generalized K-composite fading was assumed for analytical model tractability. The model is complex and considers one tier of regularly laid interfering cells. Singh et al. developed a moment-matched log-normal modeling of uplink ICI with power control and shadowing for CDMA system [33]. The aggregate uplink ICI is assumed to be log-normally distributed. The moment-matched approach was applied to OFDMA networks with sector antennas for networks without shadow fading [34]. A simplified version of the approach was used to analyze uplink performance with partial frequency reuse scheme [35]. It is noted that large network performance prediction errors are observed from the model with shadowing.

b) Stochastic geometry models: Stochastic geometry has been widely applied for cellular network performance analysis [36]–[38]. A fluid model assuming uniformly distributed BSs was used to analyze uplink ICI and uplink power compensation, but the model was not verified [39]. Norlan et al. applied the stochastic geometric tool to model OFDMA uplink ICI and network performance [22]. The model was extended by ElSawy et al. for cellular uplink transmission with truncated power control [36], [40]. Tabassum et al. modelled uplink NOMA in large-scale cellular networks using Poisson cluster processes [38]. It is noted that the stochastic geometric model for uplink transmission is not thoroughly verified by simulations and a limitation with the model is that it is not directly applicable to practical cellular network with irregular cellular shapes, or with sector antennas which may cause an interfering user to be closer to the site location than the target user.

c) Hybrid model and contributions: Tabassum et al. applied their analytical framework to analyze uplink ICI and capacity in two-tier small cell networks [41]. In the analysis macrocell BSs are assumed to have fixed locations and small cell BSs are assumed to be randomly located. The analytical model is complex and considers the generalized K-composite fading.

One common weakness of the current uplink models is that the above models are complex and do not take into account sectorized antenna patterns except [34], and practical link level performance models are not used in these models. Shadow fading, which is an inherent nature of wireless communications, is not considered in [34]. We extend our preliminary work in [23] to develop an unified and simple analytical models for LTE network uplink communications, and apply the analytical models to investigate LTE network performance with HOS deployments.

II. System Model

A. Network Layout and Resource Allocation

In this paper, we consider LTE networks with antenna configurations of 1, 3, 6 and 12 sectors per site. For the 3-sectors configuration, a clover-leaf network layout is used[1]. Using these network layouts, let us consider a cellular network with N_{sites} sites. The eNodeBs are labeled from 1 to N_{sites}. Without loss of generality eNodeB 1 is set as the target eNodeB, located at the origin (0, 0). The inter-site distance is denoted by R_{ISD}.

The number of sectors per site is denoted by N_{a}, set to 1, 3, 6 and 12 in this paper. So the total number of sectors (denoted by N_{sect}) equals $N_{\text{sites}}N_{\text{a}}$. The jth sector of the nth site is denoted by $\mathcal{A}_{s,j}$, where $s \in [1, N_{\text{sites}}]$ and $j \in [1, N_{\text{a}}]$. For ease of notation, sector $\mathcal{A}_{s,j}$ and its sector antenna (SA) are also labeled by n, with $n = (s-1)N_{\text{a}} + j$, $s \in [1, N_{\text{sites}}]$, $j \in [1, N_{\text{a}}]$, and $n \in [1, N_{\text{sect}}]$. Let $\vartheta_{s,j}$ denotes the horizontal angle of the main radiation direction of sector $\mathcal{A}_{s,j}$, which is set to $(j-1)*\pi/N_{\text{a}} - \vartheta_{s,1}$ for ($j \in [2, N_{\text{a}}]$), with $\vartheta_{s,1} = -\pi/6$ for the 3-sectors and $-\pi/12$ for the 6-sectors and 12-sectors settings, respectively.

In LTE networks single carrier frequency division multiple access (SC-FDMA) is chosen for uplink multiple access. SC-FDMA has most of the merits of OFDMA but has a lower peak to average power ratio (PAPR). With SC-FDMA spectrum resources are split up into a number of parallel orthogonal narrow-band sub-carriers with a space of 15 kHz, which are then organized into resource blocks for allocation. An LTE uplink radio frame consists of 20 slots of 0.5 ms each, and one subframe consists of two slots. Each slot carries either 6 or 7 SC-FDMA symbols for short and long cyclic prefix (CP) configurations, respectively. The resource grid for the uplink comprises a number of resource blocks in the frequency-time domains. The minimum resource for allocation has a granularity of 1 ms in time domain and a granularity of 180 kHz (i.e., 12 subcarriers) in frequency domain. The eNodeB allocates unique time-frequency resources to users, which eliminates intra-cell interference but not inter-cell interference. For ease of notation, we define a physical resource block (PRB) as the minimum resource used for transmission with 180 kHz by one symbol.

We assume a round-robin scheduler for resource allocation. A universal frequency reuse scheme is used, which means the available network frequency resource is used by every sector of the eNodeBs. We assume a fully loaded network, in which all the available resource blocks are allocated to the users in the

[1]For the 3-sectors BS case, the clover-leaf network layout was found to have a better performance than the hexagonal network layout [42].

This article has been accepted for publication in a future issue of this journal, but has not been fully edited. Content may change prior to final publication. Citation information: DOI 10.1109/TVT.2019.2940460, IEEE Transactions on Vehicular Technology

sectors. Users are assumed to be uniformly distributed within the network.

Table I lists the main notations used in this paper.

B. Channel Model and Antenna Radiation Pattern

Since we consider a fully loaded network, without loss of generality, we can focus our study on one sector (say sector 1) by investigating the performance of users located in sector 1 with one PRB.

Let us consider a general user u_k served by sector k, where $k \in [1, N_{\text{sect}}]$.

Define the signal power $\mathcal{P}_{n,u_k}$ received by sector n from a user u_k , which is expressed by:

$$\mathcal{P}_{n,u_k} = P^{\text{t}}_{u_k} G_{\text{PL}}(n,u_k) G_{\text{A}}(n,u_k) \psi_{n,u_k}, \tag{1}$$

where $P^{\text{t}}_{u_k}$ is the transmit power from user u_k over a PRB, $G_{\text{PL}}(n,u_k)$ is the path loss between the site of sector n and user u_k, $G_{\text{A}}(n,u_k)$ is the antenna gain between sector n and user u_k, and ψ_{n,u_k} is the shadow fading between sector n and user u_k. For ease of notation, we let P^{r}_{n,u_k} denote the received power by sector n from user u_k without shadowing:

$$P^{\text{r}}_{n,u_k} = P^{\text{t}}_{u_k} G_{\text{PL}}(n,u_k) G_{\text{A}}(n,u_k). \tag{2}$$

The antenna gain $G_{\text{A}}(n,u_k)$ models the gain of the antenna in the direction between sector n and user u_k:

$$G_{\text{A}}(n,u_k) = G_{\text{A,max}} G_{\text{A,h,v}}(\vartheta_{n,u_k}, \theta_{n,u_k}), \tag{3}$$

where $G_{\text{A,max}}$ is the maximum antenna gain, and $G_{\text{A,h,v}}(\vartheta,\theta)$ is the 3-dimensional antenna radiation pattern with horizontal angle ϑ and vertical angle θ between a considered pair of sector and user.

The shadow fading ψ_{n,u_k} models the variability of the path loss between sector n and user u_k, which is assumed to follow a log-normal distribution. According to [43], the Gaussian random variables that characterize the log-normal shadowing are assumed to have a zero mean and a standard deviation of σ_{w}. For simplicity, the shadowing between users and the sectors is assumed to be uncorrelated.

C. Fractional Power Control

Uplink power control has a great impact on achieving a required SINR, while at the same time controlling the interference caused to neighboring cells. In a classic power control scheme, all users are expected to receive the same SINR in uplink. An alternative power control scheme, FPC, which was approved by 3GPP, is used in the paper. With the FPC scheme users with a higher path loss can operate at a lower SINR and thus generate less inter-cell interference [21].

Suppose that the path loss and the antenna gain between a general user u_n and its serving sector is $G_{\text{PL}}(n,u_n)$ and $G_{\text{A}}(n,u_n)$, respectively. According to the FPC and the aforementioned notations, we can use the following formula to determine the transmit power from the user u_n:

$$P^{\text{t}}_{u_n} = \min\Big(P_{\max}, P_{\text{target}} M \Big[G_{\text{PL}}(n,u_n) G_{\text{A}}(n,u_n)\Big]^{-\beta}\Big), \tag{4}$$

where β is the power compensation factor [21], taking values of 0, 0.4 to 1 with a step of 0.1; M is the number of PRBs allocated to a user, which is set to 1 in this paper. $P_{\max}$ is the maximal uplink transmit power on a PRB, and P_{target} is a configurable target received power.

III. SINR Expression and Existing Analytical Models

A. General Expression of SINR

As assumed in Section II, we focus our analysis on the performance of users associated with sector 1, based on which the overall network performance can be calculated.

Taking into account the previous definitions, the SINR (denoted by γ_{u_1}) for a general target user u_1 within sector 1 can be calculated as:

$$\gamma_{u_1} = \frac{\mathcal{P}_{1,u_1}}{\sum\limits_{n=2}^{N_{\text{sect}}} \mathcal{P}_{1,u_n} + \delta^2} = \frac{P^{\text{r}}_{1,u_1}\psi_{1,u_1}}{\sum\limits_{n=2}^{N_{\text{sect}}} P^{\text{r}}_{1,u_n}\psi_{1,u_n} + \delta^2}, \tag{5}$$

where δ^2 is the noise power.

As shadow fading ψ_{1,u_n} is assumed to be independent for all users u_n within sector n, we can use ψ_n to represent the shadow fading between any interfering user u_n from sector n and sector 1, and rewrite the expression in (5) for SINR:

$$\gamma_{u_1} = \frac{P^{\text{r}}_{1,u_1}\psi_{1,u_1}}{\sum\limits_{n=2}^{N_{\text{sect}}} P^{\text{r}}_{1,u_n}\psi_n + \delta^2}. \tag{6}$$

Let I_n denote the uplink ICI generated from sector n ($2 \le n \le N_{\text{sect}}$) without shadowing, and its mean and variance denoted by $\overline{I}_n$ and $\widehat{I}_n$ respectively. The mean and variance of I_n will be calculated in Section IV. Let $I_{\text{w},n}$ denote the uplink ICI generated from sector n ($2 \le n \le N_c$) with shadowing. We have $I_{\text{w},n} = I_n\psi_n$. Let I_{sum} denote the sum of the single sector interference $I_{\text{w},n}$ ($2 \le n \le N_{\text{sect}}$), which is $I_{\text{sum}} = \sum_{n=2}^{N_{\text{sect}}} I_{\text{w},n}$. Let $\overline{I}_{\text{sum}}$ and $\widehat{I}_{\text{sum}}$ denote the mean and variance of I_{sum}.

With the above definitions for the uplink ICI, the expression in (6) for SINR can be further rewritten as:

$$\gamma_{u_1} = \frac{P^{\text{r}}_{1,u_1}\psi_{1,u_1}}{\sum\limits_{n=2}^{N_{\text{sect}}} I_n\psi_n + \delta^2} = \frac{P^{\text{r}}_{1,u_1}\psi_{1,u_1}}{I_{\text{sum}} + \delta^2}. \tag{7}$$

B. Existing Analytical Models

The main challenge of modeling uplink interference and network performance comes from the dynamic positions of the interfering users. Although the moments of single cell interference I_n has been computed and used in the literature (such as mean and variance), there is no simple and well-established model proposed to approximate the distribution of I_n, which hinders the development of effective analytical models for uplink communications of LTE and other OFDMA based cellular networks. In this subsection we briefly discuss two existing analytical approaches used for uplink communications of cellular networks.

This article has been accepted for publication in a future issue of this journal, but has not been fully edited. Content may change prior to final publication. Citation information: DOI 10.1109/TVT.2019.2940460, IEEE Transactions on Vehicular Technology

TABLE I
NOTATIONS

Notation	Meaning	Notation	Meaning
N_{site}	Number of sites	R_{ISD}	Inter-site distance
N_{a}	Number of sectors per BS	N_{sect}	Total number of sectors
$\mathcal{A}_{n,j}$	jth sector of nth site (j = 1,...,N_{a})	$\mathcal{A}_k$	Sector k or $\mathcal{A}_{n,j}$, k=$(n-1)N_{\text{a}}+j$
$\mathcal{P}_{n,u_k}$	receive power by sector n from u_k	$P^{\text{t}}_{u_n}$	transmit power over PRB fromu_n
P_{max}	maximal transmit power over a PRB	P_{target}	target rec power at eNodeB
P^{r}_{n,u_k}	mean rec power by sector n from u_k	β	uplink power compensation factor
$G_{\text{PL}}(n,u_k)$	path loss btw. sector n and user u_k	$G_{\text{A}}(n,u_k)$	antenna gain btw. $\mathcal{A}_n$ and u_k
$G_{\text{A,max}}$	maximum antenna gain	$G_{\text{A,h,v}}(\vartheta,\theta)$	antenna radiation pattern with ϑ, θ
ϑ_{3dB}, θ_{3dB}	horizontal and vertical HPBW	δ^2	noise power
ψ_{n,u_k}	shadowing between sector n and u_k	σ_{w}	shadowing standard deviation (std)
I_n	sector n ICI without shadowing	$\overline{I_n}$, $\widehat{I_n}$	mean and variance of I_n
$I_{\text{w},n}$	sector n ICI with shadowing	$\mu_{I_{\text{w},n}}$, $\sigma_{I_{\text{w},n}}$	mean, std of logarithm of $I_{\text{w},n}$
I_{sum}	aggregate ICI to sector 1	$\overline{I_{\text{sum}}}$, $\widehat{I_{\text{sum}}}$	mean, variance of I_{sum}
μ_{I_n}, σ_{I_n}	mean, std of logarithm of I_n	$\mu_{I_{\text{sum}}}$, $\sigma_{I_{\text{sum}}}$	mean, std of logarithm of I_{sum}
γ_{u_k}	SINR of user u_k from sector k	$\overline{\gamma_u}$, $\widehat{\gamma_u}$	mean, variance of SINR of user u
μ_{γ_u}, σ_{γ_u}	mean, std of natural logarithm of γ_u	γ_{net}, η_{site}, $\mathcal{O}_{\text{net}}$	SINR, site throughput, outage prob.

1) Moment Matching Analytical Model: An analytical approach was originally proposed to model the uplink ICI for cellular networks with assumption of multiple intra-cell and inter-cell interferers [33]. Shadow fading, power control and cell association were taken into account in the analytical model. The approach was applied in [34] to evaluate interference and network throughput of OFDMA cellular networks with fractional frequency reuse but without considering shadowing and power control.

The main idea used in this approach is that the aggregate ICI I_{sum} is approximated as a log-normal random variable, without any assumption on the distribution of the single cell ICIs. According to the log-normal assumption for I_{sum}, I_{sum} can be uniquely characterised by its mean and variance ($\overline{I}_{\text{sum}}$ and $\widehat{I}_{\text{sum}}$). To determine the mean and variance of I_{sum}, a moment matching method was proposed in [33] to match the mean and variance of I_{sum} to the values which are related to the mean and variance of single sector ICIs.

Once the mean and variance ($\overline{I}_{\text{sum}}$ and $\widehat{I}_{\text{sum}}$) of the aggregate ICI I_{sum} are computed, we can compute the mean network-wide spectrum efficiency and throughput with the method presented in Section IV. The analytical model based on the idea of moment matching for the aggregate ICI in [33] [34] is called moment matching model (MoM model) in this paper.

2) Sum of Means Analytical Model: In this model shadowing is not considered [35]. The mean of single sector ICI is simply summed up to approximate the aggregate ICI I_{sum}. Then the SINR for a given user u_1 without shadowing is computed by the following formula:

$$\gamma_{u_1} = \frac{P^{\text{r}}_{1,u_1}}{\sum_{i=2}^{N_{\text{sect}}} I_i + \delta^2} \approx \frac{P^{\text{r}}_{1,u_1}}{\sum_{i=2}^{N_{\text{sect}}} \overline{I}_n + \delta^2}. \tag{8}$$

From (8), mean network-wide spectrum efficiency and throughput can be computed. This simple analytical model with the approach of summing up the mean single sector ICI as the aggregate ICI is called sum of means (SoM) model.

IV. PROPOSED ANALYTICAL MODELS

A. Uplink ICI Observation and General Framework

Through network simulations it is observed that the MoM and SoM analytical models can be used for system performance evaluation of cellular networks without shadowing, but the models show poor performance when shadowing is taken into account.

In [23] the single cell ICIs with shadowing was assumed to follow log-normal distribution in the case of omni-directional antennas, which enables simple analytical modeling of OFDMA based cellular networks. Next we investigate how well the single sector ICIs and aggregate ICI with shadowing can be approximated by log-normal random variables.

Multi-cell simulations were run to obtain the values of the single sector and the aggregate ICI with shadowing (8 dB σ_{w}), for the four antenna settings: 1, 3, 6 or 12 sector antennas per site N_{a}, with R_{ISD}=500 m, and power compensation factor $\beta = 0.4$. The number of samples N_{sp} for each setting on N_{a} is 20000. Representative results on the log-normal fit to the single sector ICIs (from sectors 3, 6, 9 and 12) for the 3 sectors per site setting are presented in Fig. 1. Log-normal fittings to the aggregate ICI for the four N_{a} settings are presented in Fig. 2. It can be observed from the histogram plots that the fittings for the single sector and aggregate ICIs by log-normal distributions are good.

Furthermore, we measure the goodness of fit quantitatively on the simulated single sector ICIs by log-normal distribution with the Anderson-Darling (AD) test [44]. The key of the AD test is the computation of the AD statistic value (denoted by AD_n for the nth sector ICI test) with the following formula [44]:

$$AD_n = -N_{\text{sp}} - \sum_{i=1}^{N_{\text{sp}}} \frac{2i-1}{N_{\text{sp}}} \Big\{ \ln[F(Y_{n,i})] + \ln[1 - F(Y_{n,N_{\text{sp}}-i+1})] \Big\} \tag{9}$$

where N_{sp} denotes the number of samples used in an AD test, $Y_{n,i}$ denotes the ith data of the ordered simulated ICI

This article has been accepted for publication in a future issue of this journal, but has not been fully edited. Content may change prior to final publication. Citation information: DOI 10.1109/TVT.2019.2940460, IEEE Transactions on Vehicular Technology

samples from sector n, $\ln(x)$ is the natural logarithm function, $F(x)$ denotes the cumulative distribution function for the log-normal distribution. The distribution parameters for the hypothesized log-normal distribution are estimated from the simulation sector ICI samples. For a given critical value, if the computed AD statistic value AD_n is smaller than a specific critical value, then the hypothesis H_1 that the sector n ICI comes from the hypothesized log-normal distribution can be accepted. The critical value for AD test is dependent on the significance level [44], for example the widely used significance levels of 1% and 5% gives critical values of 1.035 and 0.752, respectively.

The above AD test procedure is applied to all the interfering sectors as well as the sector of interest (i.e. Sector 1) separately for the four N_{a} settings. The AD statistic values for the received power by Sector 1 and all the interfering sector ICIs are presented in Fig. 3(d). Comparing the AD statistic values of the sectors to the critical value 1.035, we can confirm that a large majority of sector ICIs follow log-normal distribution, and the remaining sectors have ICIs closely following log-normal distribution. For example, for the case of N_{a}=1, the AD value for 14 out of the 18 interfering sectors is less than the critical value, and the other 4 sectors also have an AD value of less than 1.6. For the case of N_{a}=3, the AD value for 51 out of 56 sectors is smaller than 1.035, which means 51 sector ICIs follow log-normal distribution according to the AD test.

According to the experiment results, we can make the following assumption with high confidence: the single sector ICIs with shadowing ($I_{\text{w},n}$ for $n \in [2, N_{\text{sect}}]$) are independent log-normal random variables.

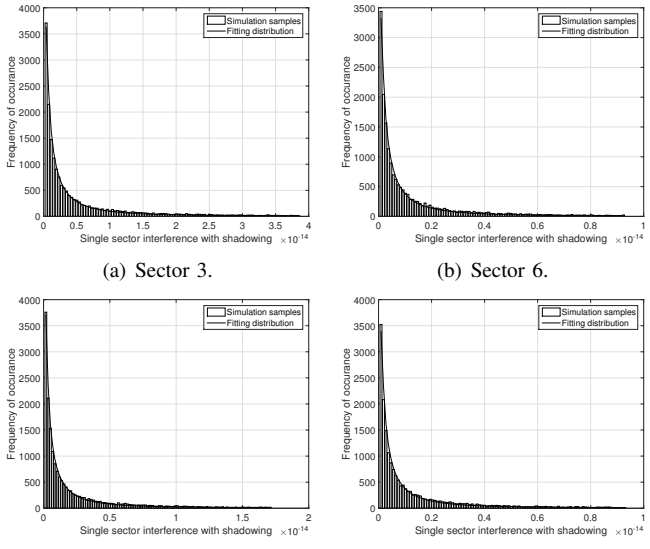

(a) Sector 3. (b) Sector 6.

(c) Sector 9. (d) Sector 12.

Fig. 1. Density of single sector ICIs with 8 dB shadowing with the 3 sectors per site setting, from a) sector 3; b) sector 6; c) sector 9 and d) sector 12. β=0.4.

With the assumption of the single sector ICIs being log-normal random variables, the aggregate ICI can be approximated by a log-normal random variable with widely used

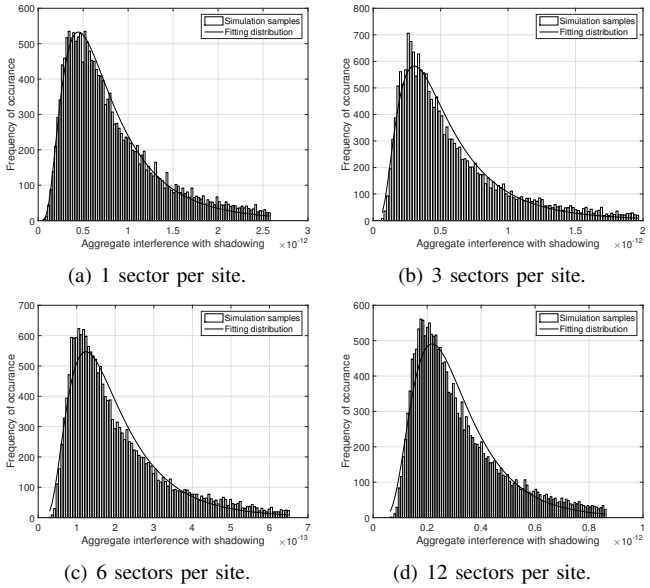

(a) 1 sector per site. (b) 3 sectors per site.

(c) 6 sectors per site. (d) 12 sectors per site.

Fig. 2. Log-normal fitting of aggregate ICI with 8 dB shadowing, under different settings on the number of sectors per site N_{a} of : a) 1; b) 3; c) 6; and d) 12. $\beta = 0.4$.

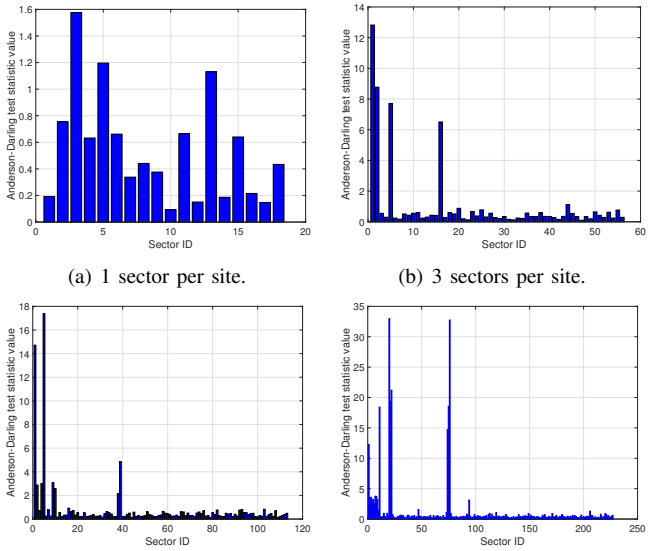

(a) 1 sector per site. (b) 3 sectors per site.

(c) 6 sectors per site. (d) 12 sectors per site.

Fig. 3. AD test statistic value of sector ICIs with 8 dB shadowing, under different settings on the number of sectors per site N_{a} of : a) 1; b) 3; c) 6; and d) 12. $\beta = 0.4$.

analytical tools for addition of multiple log-normal random variables.

Next we propose two analytical approaches to compute the single sector ICI $I_{\text{w},n}$ for a general sector n, based on which two analytical models are developed correspondingly to compute system level performance metrics of interest. The two proposed analytical models are called log-normal mean (LoM) model and log-normal log-normal (LoL) model, respectively. With both LoM and LoL models the aggregate ICI is approximated by a log-normal random variable. But the single sector ICIs without shadowing are modelled by their means in the LoM model and by log-normal random variables

This article has been accepted for publication in a future issue of this journal, but has not been fully edited. Content may change prior to final publication. Citation information: DOI 10.1109/TVT.2019.2940460, IEEE Transactions on Vehicular Technology

in the LoL model, respectively. More details on the LoM and LoL models are presented later.

The overall analytical framework based on the proposed analytical models is shown in Fig. 4. It is general and can take into account various cellular deployment geometries, antenna radiation patterns, channels models, user distributions, and link performance models. According to the received signal strength from the sectors in the network, users are first associated to the sector with the strongest received signal. Then we can compute the single sector ICIs and the aggregate ICI. The aggregate ICI model combined with given link performance models can be used to compute network performance metrics of interest.

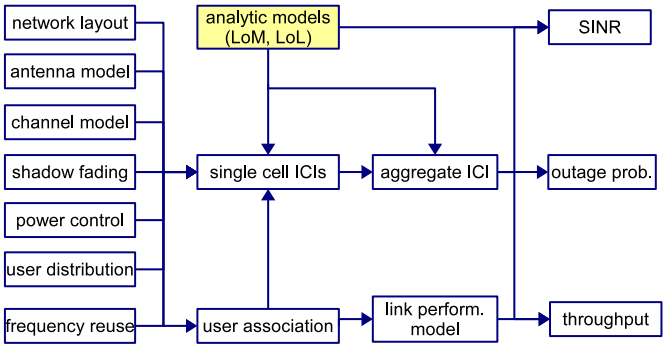

Fig. 4. General analytical framework.

a) LoM Model: In the analytical model LoM, $I_{\mathrm{w},n}$ (for $n \in [2, N_{\mathrm{sect}}]$) is approximated by the product of the mean of I_n and the shadowing ψ_n:

$$I_{\mathrm{w},n} \approx \overline{I}_n \psi_n. \tag{10}$$

As the mean of single sector ICI without fading is a deterministic variable and the shadowing is a log-normal variable, it is easy to compute the mean and variance of the single sector ICI $I_{\mathrm{w},n}$with shadowing as a log-normal random variable. Then the aggregate ICI as a sum of the log-normal approximated ICI from multiple sectors is also approximated as a log-normal random variable.

b) LoL Model: The LoM model is simple and has much higher accuracy than the MoM and SoM models, but the prediction error is still large when shadowing is present. In the second analytical model, the single sector ICIs without shading are also approximated by log-normal random variables.

B. Approaches to Compute Single Sector ICI $I_{w,n}$

For a general log-normal variable x, it can be uniquely characterised by the mean μ and standard deviation σ for the variable x's natural logarithm. The probability density function $f_{\mathrm{LN}}(x; \mu, \sigma)$ of the log-normal variable x can be expressed by:

$$f_{\mathrm{LN}}(x; \mu, \sigma) = \frac{1}{x\sigma\sqrt{2\pi}} \mathrm{e}^{-\frac{(\ln x - \mu)^2}{2\sigma^2}}. \tag{11}$$

Let $\mu_{w,n}$ and $\sigma_{w,n}$ denote the mean and standard deviation of the normal logarithm of $I_{w,n}$. Next we present the approaches to determine the key parameters $\mu_{w,n}$ and $\sigma_{w,n}$ for the log-normal distribution associated with the single sector ICI $I_{w,n}$, used in the LoM and LoL models, respectively.

1) Computation of Mean and Variance of I_n: Let ρ_n denote the user density in sector n, $n \in [1, N_{\mathrm{sect}}]$. With the assumption of uniform user locations, we have $\rho_n = \frac{1}{\text{area of sector } n}$. At a given time, consider a general user u_n served by sector n. With given locations for user u_n, sector 1 (target sector) and sector n, we can compute the distance D_{1,u_n} between user u_n and sector 1 and the distance D_{n,u_n} between user u_n and sector n. Then the interference contributed from user u_n of sector n can be computed with P^{r}_{1,u_n} from (2).

Without loss of generality, suppose user u_n is located with polar coordinates (r_n, θ_n) relative to its serving sector (sector n). The mean and variance of single sector ICI I_n can be computed by integrating the interference contributed from user u_n over sector n, for $n = 2, ..., N_{\mathrm{sect}}$:

$$\overline{I}_n = \iint_{\mathcal{A}_n} P^{\mathrm{r}}_{1,u_n} \rho_n r_n \mathrm{d}r_n \mathrm{d}\theta_n, \tag{12}$$

$$\widehat{I}_n = \iint_{\mathcal{A}_n} \left(P^{\mathrm{r}}_{1,u_n} - \overline{I}_n\right)^2 \rho_n r_n \mathrm{d}r_n \mathrm{d}\theta_n, \tag{13}$$

where P^{r}_{1,u_n} is a function of u_n coordinates (r_n, θ_n). The integrals (12) and (13) can be calculated by traditional numerical quadrature tools.

2) LoM Model: With the approximation used for LoM model, we can compute $\mu_{\mathrm{w},n}$ and $\sigma_{\mathrm{w},n}$ for $I_{\mathrm{w},n}$ for analytical model LoM using the following approach:

$$\mu_{\mathrm{w},n} = \log(\overline{I}_n), \tag{14}$$

$$\sigma^2_{\mathrm{w},n} = \sigma^2_{\mathrm{w}}. \tag{15}$$

3) LoL Model: With LoL model, single sector ICIs without shadowing are also assumed to be log-normal variables. Let μ_n and σ_n^2 denote the mean and variance of the natural logarithm of I_n, for $n \in [2, N_{\mathrm{sect}}]$, respectively. μ_n and σ_n^2 can be calculated from $\overline{I}_n$ and $\widehat{I}_n$ by:

$$\sigma_n^2 = \ln\left(1 + \frac{\widehat{I}_n}{\overline{I}_n}\right), \tag{16}$$

$$\mu_n = \ln(\overline{I}_n) - \frac{\sigma_n^2}{2}. \tag{17}$$

As single sector ICI with shadowing is approximated by the product of two log-normal random variable in LoL model, we can compute $\mu_{\mathrm{w},n}$ and $\sigma_{\mathrm{w},n}$ for $I_{\mathrm{w},n}$ for LoL model:

$$\mu_{\mathrm{w},n} = \mu_n, \tag{18}$$

$$\sigma^2_{\mathrm{w},n} = \sigma_n^2 + \sigma^2_{\mathrm{w}}. \tag{19}$$

Now we can see the main difference between LoM model and LoL model: for LoM model, formulas (14) and (15) are used to compute $\mu_{\mathrm{w},n}$ and $\sigma_{\mathrm{w},n}$ of $I_{\mathrm{w},n}$; whereas for LoL model formulas (18) and (19) are used.

C. Aggregate Interference I_{sum}

The aggregate interference I_{sum} is the sum of the single sector ICIs from the interfering sectors (independent log-normally distributed random variables). There is no closed-form expression for the distribution of I_{sum}, but it can be reasonably approximated by another log-normal distribution

This article has been accepted for publication in a future issue of this journal, but has not been fully edited. Content may change prior to final publication. Citation information: DOI 10.1109/TVT.2019.2940460, IEEE Transactions on Vehicular Technology

(e.g., with commonly used Fenton method [45] or Schwartz-Yeh method [46]).

Let μ_{sum} and σ_{sum} denote the mean and standard deviation of the normal logarithm of I_{sum}, respectively, which can be computed according to Fenton method [45].

Then from μ_{sum} and σ_{sum}, the mean (denoted by $\overline{I}_{\text{sum}}$) and variance (denoted by $\widehat{I}_{\text{sum}}$) of the aggregate ICI I_{sum} can be obtained by:

$$\overline{I}_{\text{sum}} = e^{\mu_{\text{sum}}+\sigma^2_{\text{sum}}/2}, \quad (20)$$

$$\widehat{I}_{\text{sum}} = (e^{\sigma^2_{\text{sum}}}-1)\overline{I}_{\text{sum}}. \quad (21)$$

D. SINR and Network Throughput

Statistically users located in the target sector (sector 1) experience the aggregate ICI following the same log-normal distribution. Without loss of generality, let us consider a general user u in the target sector. The SINR γ_u for user u is calculated as:

$$\gamma_u = \frac{\mathcal{P}_{1,u}}{I_{\text{sum}}+\delta^2}. \quad (22)$$

Let $\mathcal{V}_{\text{IN}} = I_{\text{sum}} + \delta^2$. For model tractability, δ^2 is treated as a log-normal variable with mean of $\log(\delta^2)$ and standard deviation of 0 for its logarithm. Then we can approximate $\mathcal{V}_{\text{IN}}$ by a new log-normal variable, with mean and standard deviation denoted by μ_{IN} and σ_{IN} for its logarithm, respectively. μ_{IN} and σ_{IN} can be calculated by Fenton approximation method again [45].

Now as $\mathcal{P}_{1,u}$ and $\mathcal{V}_{\text{IN}}$ are modelled as two independent log-normal variables, the SINR γ_u of user u can be modelled as a log-normal variable. Let μ_{γ_u} and σ_{γ_u} denote the mean and standard deviation of the normal distribution associated with γ_u, which can be computed according to the properties of log-normal random variables by the following formulas:

$$\mu_{\gamma_u} = \ln(P^{\text{r}}_{1,u}) - \mu_{\text{IN}}, \quad (23)$$

$$\sigma^2_{\gamma_u} = \sigma^2_w + \sigma^2_{\text{IN}}. \quad (24)$$

Let $\overline{\gamma}_u$ and $\widehat{\gamma}_u$ denote the mean and variance of SINR of user u, respectively, which can be computed using formulas similar to (20) and (21):

$$\overline{\gamma}_u = e^{\gamma_u+\gamma^2_u/2}, \quad (25)$$

$$\widehat{\gamma}_u = (e^{\gamma^2_u}-1)\overline{\gamma}_u. \quad (26)$$

Let (r,θ) denote the polar coordinates of a general user u from sector 1. The network-wide mean SINR (denoted by γ_{net}) can be obtained by integration of single user SINR γ_u over sector 1:

$$\gamma_{\text{net}} = \iint_{\mathcal{A}_{1,1}} \gamma_u \rho_1 r \mathrm{d}r\mathrm{d}\theta. \quad (27)$$

It is noted that γ_u is a function of coordinates (r,θ) of user u.

For a user with an instantaneous SINR γ_u, we suppose that there is a link layer performance model $\mathcal{F}(.)$ that can map a SINR γ_u to spectral efficiency (bps/Hz). Let $\mathcal{C}_u$ and $\overline{\mathcal{C}}_u$ denote the instantaneous and average spectrum efficiency (bps/Hz) of user u, respectively, which are calculated by:

$$\mathcal{C}_u = \mathcal{F}(\gamma_u), \quad (28)$$

$$\overline{\mathcal{C}}_u = \int_0^\infty \mathcal{F}(x) f_{\text{LN}}(x;\mu_{\gamma_u},\sigma_{\gamma_u})\mathrm{d}x. \quad (29)$$

Let $\mathcal{C}_{\text{net}}$ denote the average spectrum efficiency (bps/Hz) of sector $\mathcal{A}_1$ which is calculated by:

$$\mathcal{C}_{\text{net}} = \iint_{\mathcal{A}_{1,1}} \overline{\mathcal{C}}_u \rho_1 r \mathrm{d}r\mathrm{d}\theta. \quad (30)$$

The mean site throughput (denoted by η_{site}) in bps can be computed with network bandwidth B_{net} by:

$$\eta_{\text{site}} = N_a \mathcal{C}_{\text{net}} B_{\text{net}}. \quad (31)$$

Suppose that a user is out of service if its instantaneous SINR is lower than a given outage threshold γ_{out}. Let $\mathcal{O}_u$ and $\mathcal{O}_{\text{net}}$ denote the outage probability of the general user u, which can be calculated by:

$$\mathcal{O}_u = \int_0^{\gamma_{\text{out}}} f_{LN}(x;\mu_{\gamma_u},\sigma_{\gamma_u})dx, \quad (32)$$

$$\mathcal{O}_{\text{net}} = \iint_{\mathcal{A}_{1,1}} \mathcal{O}_u \rho_1 r \mathrm{d}r\mathrm{d}\theta. \quad (33)$$

V. Numeric Results

A. System Configurations

Analytical results are obtained with Matlab numerical tools, while simulation results are obtained by system level simulator and averaged over 10^5 simulations runs. The simulator is written in Matlab by the authors following the simulation framework of the Vienna LTE simulator developed for downlink communications [16]. Table II presents the most relevant system parameters. In the simulations, users are uniformly distributed in the networks and are associated to the sector with the strongest received signal among all the sectors. The same given channel model, antenna radiation pattern, power control strategies, and LTE link level performance model are used for both simulation and modelling. It is noted that the proposed analytical models are general and can be used with other system configurations.

The path loss model specified in [43] for outdoor line-of-sight communications is used,

$$G_{\text{PL}}(d) = -34.02 - 22\log_{10}(d)\ [\text{dB}]. \quad (34)$$

where d is the distance between a consider pair of an eNodeB site and a user.

We use the radiation pattern $G_{\text{A,h,v}}(\vartheta,\theta)$ provided in [43]:

$$G^{\text{dB}}_{\text{A,h,v}}(\vartheta,\theta) = -\min(-(G^{\text{dB}}_{\text{A,h}}(\vartheta)+G^{\text{dB}}_{\text{A,v}}(\theta)), G^{\text{dB}}_{\text{Front}}),$$

$$G_{\text{A,h,v}}(\vartheta,\theta) = 10^{G^{\text{dB}}_{\text{A,h,v}}(\vartheta,\theta)/10}. \quad (35)$$

where $G_{\text{A,h}}(\vartheta_{i,j,u})$ and $G_{\text{A,v}}(\theta_{i,j,u})$ are the normalized horizontal and vertical radiation pattern offset of the considered sector antenna, and $G^{\text{dB}}_{\text{Front}}$ is the antenna front to back ratio.

This article has been accepted for publication in a future issue of this journal, but has not been fully edited. Content may change prior to final publication. Citation information: DOI 10.1109/TVT.2019.2940460, IEEE Transactions on Vehicular Technology

TABLE II
SYSTEM SETTINGS

Parameters	Value	Parameters	Value
Carrier frequency	2000 MHz	Bandwidth B_{net}	5 MHz
# of sites	$N_{\text{sites}} = 19$	Inter-site distance	$R_{\text{ISD}} = 500$ m
# of sectors per site	$N_{\text{a}} = 1, 3, 6, 12$	Transmit power	P_{max}=250 mW
Antenna height	25 m	Target receive power	P_{target} = -50 dBm
User height	1.5 m	Antenna gain (dBi)	2, 15.5, 19.8, 22 for 1, 3, 6, 12 sectors
Front to back ratio	25 dB	Horizontal HPBW ϑ_{3dB}	65°, 33° , 17° for 3, 6, 12 sectors
Antenna mode	2x2 antennas	Vertical HPBW θ_{3dB}	11.5° , 8.5° , 8.5° for 3, 6, 12 sectors
Shadowing std dev	8 dB [43]	Antenna downtilt θ_{down}	10.38° , 8.28° , 8.28° for 3, 6, 12 sectors
Noise power	-116 dBm per PRB.	Power compensation	0, 0.4 to 1 with step of 0.1
User density (sim)	1 user over 25 m^2	Outage threshold γ_{out}	-5 dB

$G_{\text{A,h}}(\vartheta_{i,j,u})$ and $G_{\text{A,v}}(\theta_{i,j,u})$ are approximated as [43]:

$$G^{\text{dB}}_{\text{A,h}}(\vartheta) = -\min(\frac{12|\vartheta|}{\vartheta_{\text{3dB}}}, 25), \quad (36)$$

and

$$G^{\text{dB}}_{\text{A,v}}(\theta) = -\min(\frac{12|\theta - \theta_{\text{down}}|}{\theta_{\text{3dB}}}, 20), \quad (37)$$

where ϑ_{3dB} and θ_{3dB} are the horizontal and vertical half-power beamwidth (HPBW), and θ_{down} is the down-tilt angle. The values for the antenna parameters are shown in Table II.

For the numerical evaluation, we use a spectral efficiency function $\mathcal{F}(x)$, which approximates an abstracted LTE link level model developed from the LTE link level Simulator [16], with 2x2 antenna mode, open loop spatial multiplexing (OLSM) and adaptive modulation and coding (AMC). The original LTE link model (presented in Fig.9 of [16]) mapping channel SNR (dB) to spectral efficiency (bps/Hz) is approximated by a polynomial function presented in [14].

B. Network Performance with Regular Cellular Layout

Fig. 5(a), Fig. 5(b) and Fig. 5(c) present the network performance (obtained by simulations and the proposed analytical model LoL), in terms of mean network SINR (dB), mean site throughput (Mbps) and mean outage probability, against the uplink power compensation factor β, for $R_{\text{ISD}} = 500\,\text{m}$ and $\sigma_{\text{w}} = 8$ dB, respectively. The number of sectors per eNodeB is set to 1, 3, 6 and 12 in the experiments.

Table III provides more details about the mean site throughput for different system configurations. In Table III, the row with labels 'Sim' shows the site throughput obtained by simulations with various numbers of sectors per site and the relative throughput gains with respect to the omni-directional antenna setting; the rows starting with model names show the site throughput obtained by different analytical models and the absolute modeling deviation in percents with respect to the simulation results.

From Fig. 5, it can be observed that analytical results with model LoL match very well to the system-level simulation results, with less than 1.5% average difference. The overall average difference between the analytical model LoL and system-level simulation results is 1.46% for the scenario of σ_{w}=8 dB. This fact shows the accuracy of the proposed analytical model, one of the main contribution of this paper. In addition, the analytical models are significantly faster than simulations. Simulations took more than 60 hours to produce the whole simulation results presented in this paper, while analytical models only took 10 minutes. The accuracy and high computation efficiency enable the use of the proposed analytical tools as an effective method to predict network performance in a fast and reliable manner. For example, optimization tools that attempt to find proper antenna orientation and down-tilt in HOS deployments can use the proposed analytical models to quickly search over different candidate configurations and find the best performing one.

a) Impact of Power Compensation and Sector Antennas: The power compensation factor β is set to 0 and from 0.4 to 1 with a step of 0.1. The impact of power compensation is obvious. The network performance (SINR, throughput and outage probability) is at the worst without power compensation (β=0), and is close to the best with full power compensation (β=1).

If we compare the settings with different number of sectors per site, it can be observed from Fig. 5 that:

- The average network SINR decreases with number of sectors per site except for the case of omni-directional antenna setting due to the larger ICI introduced by the extra sectors per site.
- The average site throughput increases with number of sectors per site due to the lager spatial reuse.
- The outage probability changes similarly as the network SINR with increasing number of sectors per site. It is noted that the setting of 3 sectors per site gives the lowest outage probability of around 0.35, which is still large and strongly indicates the use of advanced interference mitigation schemes.

It is interesting to note that doubling the number of sectors per site from 3 to 6 almost doubles the site throughput with β=1. Increasing the number of sectors per site from 6 to 12 leads to an around 50% increase of throughput (see Table III for detailed analysis of average site throughput gains). This indicates that HOS can be used as an effective way of increasing network capacity, but the throughput gains diminish with the increasing number of sectors due to stronger inter-cell interference.

b) Comparison of Analytical Models: Next we compare the proposed analytical models (LoL and LoM) to two existing models (SoM and MoM). Numerical results against power compensation factor β are presented in Fig. 6 with σ_{w} = 8 dB. It is noted that the moment-matching approach is used in [33] to compute the uplink ICI only and is used in [35] to

This article has been accepted for publication in a future issue of this journal, but has not been fully edited. Content may change prior to final publication. Citation information: DOI 10.1109/TVT.2019.2940460, IEEE Transactions on Vehicular Technology

TABLE III
MEAN SITE THROUGHPUT AND GAIN OVER OMNI-DIRECTIONAL ANTENNA SETTING

Throughput (Mbps) and gains (%) (for simulation results) or modelling deviation (%) (for analytical model results)								
β	0.4				1			
	$N_a = 1$	$N_a = 3$	$N_a = 6$	$N_a = 12$	$N_a = 1$	$N_a = 3$	$N_a = 6$	$N_a = 12$
Sim	2.3 / 0	11.4 / 405	17.5 / 679	26.7 / 1086	2.3 / 0	10.9 / 374	19.9 / 768	31.2 / 1264
LoL	2.3 / 1.6	11.3 / 0.6	17.7 / 0.82	27.3 / 2.5	2.3 / 2.1	10.7 / 1.4	20.1 / 1.23	31.8 / 1.9
LoM	2.2 / 4.0	10.3 / 9.4	16.1 / 8.0	25.3 / 5.3	2.2 / 2.2	9.8 / 10.2	18.6 / 6.2	29.9 / 4.3
SoM	3.4 / 49.3	15.4 / 36	25 / 42.6	41.6 / 56.0	3.4 / 50.2	14.7 / 35.6	28.5 / 43.6	48.1 / 54.1
MoM	3.2 / 43.2	17.1 / 51	27.4 / 56.5	40.2 / 50.9	3.2 / 39.2	16.6 / 52.9	30.9 / 55.4	44.2 / 41.5

compute network capacity without shadowing. The approach is extended in this paper to produce SINR and site throughput results with shadowing.

It can be observed that model LoL significantly outperforms the other models for all the investigated cases. The overall modelling deviation to the simulation results for models LoL, LoM, SoM and MoM is 1.46%, 16.9%, 43.6%, 66.8%, respectively. The accuracy of LoM model is the closest to that of LoL model. In most cases, model LoM underestimates the network throughput but the prediction is reasonably good, except at two occasions of $N_a = 6$ and $N_a = 12$ with $\beta = 0$, where throughput obtained with LoM model is much higher than the simulation one. If these two occasions are excluded, considering that $\beta = 0$ is not widely used for uplink communications, the average modelling deviation of model LoM to simulation results is 8.2%, which can be acceptable for fast performance evaluation with reduced computation complexity.

C. Network Performance with Irregular Cellular Layout

A controlled irregular cellular layout is created by introducing a random movement of $(rand - 0.5) \times 125$ meters in both x-axis and y-axis directions to all the hexagonally laid out eNodeB sites except the target eNodeB site, where $rand$ is a uniform random variable in [0,1]. Representative results for the average site throughput are presented in Fig. 7(a) with $N_a = 3$. Again model LoL produces good performance prediction for all the investigated system configurations. Model LoM gives the second best performance, while models SoM and MoM largely overestimate the network throughput. Similar trends on the site throughput with increasing number of sectors can be observed for the irregular cellular layout.

VI. CONCLUSION

In this paper we have developed a unified analytical framework to characterize and relate the uplink performance indicators with key dynamic functionalities and variables. We have proposed two analytical approaches to compute the uplink ICIs from single sectors, which are approximated as log-normal random variables. The analytical approaches have a tradeoff on computation complexity and modeling accuracy. Based on the analytical approaches two analytical models (model LoM and model LoL) have been developed to compute the network performance of interest. Compared to the two existing analytical methods which use moment matching approach for aggregated ICI and the means of single sector ICIs, the proposed analytical models have better model accuracy, which are verified by system level simulations. The average difference between the results obtained by simulations and our model LoL is less than 1.5% under the investigated system setting with inter-site distance of 500 m. The analytical models were applied to LTE network with HOS deployments with both regular and irregular cellular layouts. It has been observed that increasing the number of sectors per site can effectively improve the uplink throughput. Moving from 3-sectors to 6-sectors doubles the site throughput and moving from 6-sectors to 12-sectors gives another 50% increase. However, the capacity improvement is achieved at the cost of increased outage probability due to the high spatial reuse with HOS.

ACKNOWLEDGMENT

This project has received funding from the European Unions Horizon 2020 research and innovation programme under the Marie Skodowska-Curie grant agreement No 824019 and the FP7 grant DETERMINE under the FP7-PEOPLE-2012-IRSES grant agreement No 318906.

REFERENCES

[1] M. Shafi *et al.*, "5G: A Tutorial Overview of Standards, Trials, Challenges, Deployment, and Practice," *IEEE Journal on Selected Areas in Communications*, Vol. 35, No. 6, pp. 1201 - 1221, June 2017.

[2] S. Parkvall, E. Dahlman, A. Furuskar, M. Frenne, "NR: The New 5G Radio Access Technology," *IEEE Communications Standards Magazine*, Vol. 1, No. 4, pp. 24-30, Dec. 2017.

[3] T.Tran, A. Hajisami, P. Pandey, D. Pompili, "Collaborative Mobile Edge Computing in 5G Networks: New Paradigms, Scenarios, and Challenges," *IEEE Communications Magazine*, Vol. 55, No. 4, pp. 54 - 61, April 2017.

[4] M. Al-Kadri *et al.*, "Full-Duplex Small Cells for Next Generation Heterogeneous Cellular Networks: A Case Study of Outage and Rate Coverage Analysis," *IEEE Access*, Vol. 5, pp. 8025-8038, May 2017.

[5] A. He *et al.*, "Spectral and Energy Efficiency of Uplink D2D Underlaid Massive MIMO Cellular Networks," *IEEE Transactions on Communications*, Vol. 65, No. 9, Sept. 2017.

[6] H. Elkotby, M. Vu, "Interference Modeling for Cellular Networks Under Beamforming Transmission," *IEEE Transactions on Wireless Communications*, Vol. 16, No. 8, pp. 5201-5217, Sept. 2017.

[7] B. Hagerman *et al.*, "WCDMA 6-sector deployment- case study of a real installed UMTS-FDD network," *in Proc. of IEEE VTC'06*, 2006.

[8] A. Osseiran and A. Logothetis, "Smart antennas in a WCDMA radio network system: modeling and evaluations," *IEEE Transactions on Antennas and Propagation*, Vol. 54, No. 11, pp. 3302-3316, Nov. 2006.

[9] A. Osseiran, P. Skillermark and M. Olsson, "Multi-antenna SDMA in OFDM radio networks systems: modeling and evaluations," *in Proc. of IEEE PIMRC'07*, 2007.

[10] H. Huang *et al.*, "Increasing downlink cellular throughput with limited network MIMO coordination," *IEEE Transactions on Wireless Communications*, Vol. 8, No. 6, pp. 2983-2989, June 2009.

[11] H. Huang *et al.*, "Increasing throughput in cellular networks with higher-order sectorization," *in Proc. Asilomar'10*, 2010.

[12] I. Riedel and G. Fettweis, "Increasing throughput and fairness in the downlink of cellular systems with N-fold sectorization," *in Proc. of GlobeCom'11*, 2011.

This article has been accepted for publication in a future issue of this journal, but has not been fully edited. Content may change prior to final publication. Citation information: DOI 10.1109/TVT.2019.2940460, IEEE Transactions on Vehicular Technology

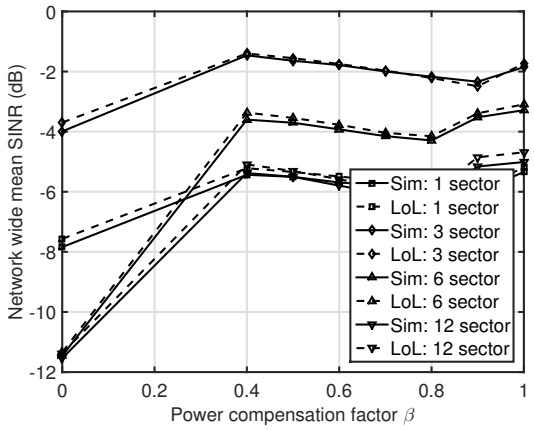

(a) Mean SINR (dB).

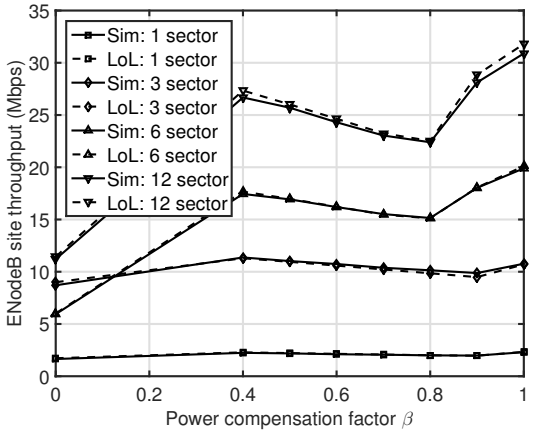

(b) Mean site throughput (Mbps).

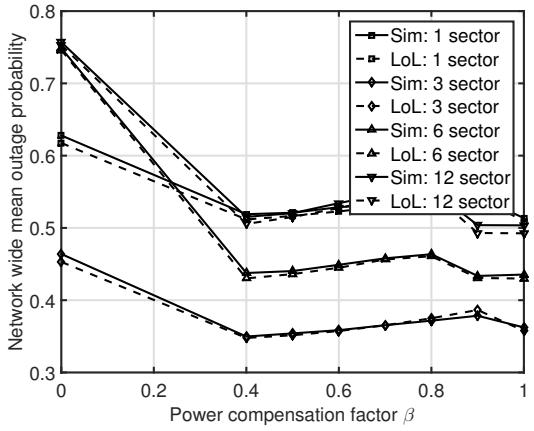

(c) Mean outage probability.

Fig. 5. Network-wide performance with different number of sector antennas. $R_{\mathrm{ISD}} = 500$ m, power compensation factor β= 1, σ_{w} = 8 dB.

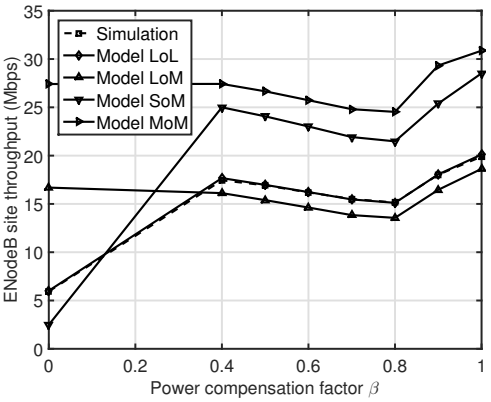

(a) $N_{\mathrm{a}} = 6$.

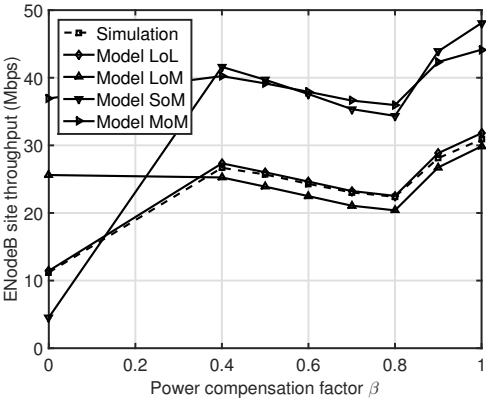

(b) $N_{\mathrm{a}} = 12$.

Fig. 6. Mean site throughput (Mbps) of various analytical models against power compensation factor β with σ_{w} = 8 dB, for a) $N_{\mathrm{a}} = 1$; b) $N_{\mathrm{a}} = 3$; c) $N_{\mathrm{a}} = 6$; d) $N_{\mathrm{a}} = 12$.

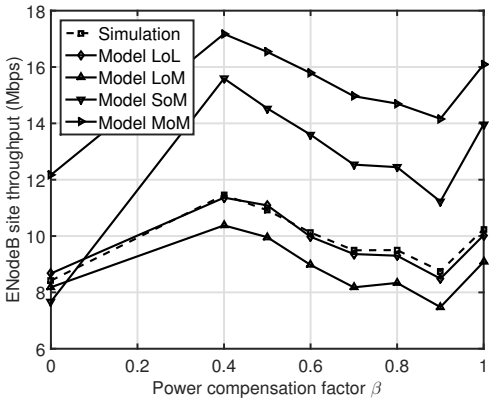

(a) Comparison of the analytical models with $N_{\mathrm{a}} = 3$.

Fig. 7. Mean site throughput (Mbps) against power compensation factor β with irregular cellular layout. σ_{w} = 8 dB.

[13] R. Joyce and L. Zhang, "Higher order horizontal sectorisation gains for a real 3GPP/HSPA+ network," *in Proc. European Wireless*, 2013.

[14] J. He *et al.*, "Analytical evaluation of higher order sectorization, frequency reuse and user classification methods in OFDMA networks," *IEEE Transactions on Wireless Communications*, Vol. 15, No. 12, pp. 8209-8222, Dec. 2016.

[15] J. Erman *et al.*, "Over The Top Video: The Gorilla in Cellular Networks," *ACM SIGCOMM*, 2011.

[16] Mehlfuhrer et al., "The Vienna LTE simulators - Enabling reproducibility in wireless communications research," *EURASIP Journal on Advances in Signal Processing*, pp.1-14, 2011:29, 2011.

[17] L. Chen *et al.*, "System-level simulation methodology and platform for mobile cellular systems," *IEEE Communications Magazine*, Vol. 49, No. 7, 2011.

[18] T. Bonald and A. Proutiere, "Wireless downlink data channels: user performance and cell dimensioning," *In Proc. Mobicom'03*, 2003.

[19] J. Andrews, F. Baccelli, and R. Ganti, "A tractable approach to coverage and rate in cellular networks," *IEEE Transactions on Communications*, Vol. 59, No. 11, pp. 3122-3134, Nov. 2011.

[20] T. Novlan, R. Ganti, A. Ghosh, J. Andrews, "Analytical evaluation of fractional frequency reuse for OFDMA cellular networks," *IEEE Transactions on Wireless Communications*, Vol. 10, No. 12, pp. 4294-4305, Dec. 2011.

[21] C. Castellanos *et al.*, "Performance of uplink fractional power control in UTRAN LTE," *In Proc. of IEEE VTC'08*, 2008.

[22] T. Norlan *et al.*, "Analytical modeling of uplink cellular networks," *IEEE Transactions on Wireless Communications*, pp.2669-2679, June 2013.

[23] J. He *et al.*, "Statistical model of OFDMA cellular networks uplink interference using Lognormal distribution," *IEEE Wireless Communications Letters*, Vol.2, No.5, pp. 575-578, Oct. 2013.

[24] B. Yang, W. Guo, Y. Jin and S. Wang, "Smartphone Data Usage: Downlink and Uplink Asymmetry", *IET Electronics Letters*, Vol. 52, No. 3, 2015.

[25] A. Wyner, "Shannon-theoretic approach to a Gaussian cellular multiaccess channel," *IEEE Transactions on Information Theory*, Vol. 40, No. 6, pp.1713-1727, Nov. 1994.

[26] J. Xu, J. Zhang, and J. Andrews, "On the accuracy of the Wyner model in downlink cellular networks," *In Proc. IEEE ICC'11*, 2011.

[27] H. Haas and S. McLaughlin, "A derivation of the PDF of adjacent channel interference in a cellular system," *IEEE Communications Letters*, Vol. 8, No. 2, Feb. 2004.

[28] Y. Zhu *et al.*, "Distribution of uplink inter-cell interference in OFDMA networks with power control," *In Proc. IEEE ICC'14*, 2014.

[29] S. Elayoubi and O. Haddada, "Uplink intercell interference and capacity in 3G LTE systems," *In Proc. IEEE ICON'07*, 2007.

[30] M. Karray, "Evaluation of the blocking probability and the throughput in the uplink of wireless cellular networks," *In Proc. IEEE ComNet'10*, 2010.

[31] H. Tabassum *et al.*, "A framework for uplink intercell interference modeling with channel-based scheduling," *IEEE Transactions on Wireless Communications*, Vol. 12, No. 1, pp. 206-219, Jan. 2013.

[32] H. Tabassum *et al.*, "A statistical model of uplink inter-cell interference with slow and fast power control mechanisms," *IEEE Transactions on Communications*, Vol. 61, No. 9, pp. 3953-3966, Sep. 2013.

[33] S. Singh *et al.*, "Moment-matched lognormal modeling of uplink interference with power control and cell selection," *IEEE Transactions on Wireless Communications*, Vol. 9, No. 3, pp. 932-938, Mar. 2010.

[34] H. Chang and I. Rubin, "Optimal downlink and uplink fractional frequency reuse in cellular wireless networks," *IEEE Transactions on Vehucular Technology*, April 2015.

[35] L. Wang *et al.*, "An analytical framework for multi-layer partial frequency reuse scheme design in mobile communication systems," *IEEE Transactions on Vehucular Technology*, Nov. 2015.

[36] H. ElSawy *et al.*, "Modeling and Analysis of Cellular Networks Using Stochastic Geometry: A Tutorial," *IEEE Communications Surveys and Tutorials*, Vol. 19, No. 1, pp. 167-203, 1st Quater 2017.

[37] M. Haenggi, "User Point Processes in Cellular Networks," *IEEE Wireless Communications Letters*, Vol. 6, No. 2, pp. 258-261, April 2017.

[38] H. Tabassum, E. Hossain, and M. Hossain, "Modeling and Analysis of Uplink Non-Orthogonal Multiple Access in Large-Scale Cellular Networks Using Poisson Cluster Processes," *IEEE Tranactions on Communications*, Vol. 65, No. 8, pp. 3555-3570, Aug. 2017.

[39] M. Coupechoux and J. Kelif, "How to set the fractional power control compensation factor in LTE?" *in Proc. of IEEE Sarnoff Symposium*, May 2011.

[40] H. ElSawy and E. Hossain, "On stochastic geometry modeling of cellular uplink transmission with truncated channel inversion power control," *IEEE Transactions on Wireless Communications*, Vol. 13, No. 8, pp. 4454-4469, Aug. 2014.

[41] H. Tabassum *et al.*, "Interference statistics and capacity analysis for uplink transmission in two-tier small cell networks: a geometric probability approach," *IEEE Transactions on Wireless Communications*, Vol. 13, No. 7, pp. 3837-3852, July 2014.

[42] M. Sheikh, and J. Lempiinen, "A flower tessellation for simulation purpose of cellular network with 12-sector sites," *IEEE Wireless Communications Letters*, Vol. 2, No. 3, pp. 279-282, June 2013.

[43] 3GPP TR 36.814 V9.0.0, "Further advancements for E-UTRA physical layer aspects, Technical Report, March 2010.

[44] N. Razali, Y. Wah, "Power comparisons of Shapiro-Wilk, Kolmogorov-Smirnov, Lilliefors and Anderson-Darling tests" *Journal of Statistical Modeling and Analytics*, Vol. 2, No. 1, pp. 2133, 2011.

[45] L. Fenton, "The sum of log-normal probability distributions in scatter transmission systems," *IEEE Transactions on Communications*, Vol. 8, No. 1, pp. 57-67, Mar. 1960.

[46] S. Schwartz and Y. Yeh, "On the distribution function and moments of power sums with lognormal components, *Bell System Technology Journal*, Vol. 61, No. 7, pp. 1441-1462, Sept. 1982.

Jianhua He received his BSc and MSc degrees from Huazhong University of Science and Technology (HUST), China, and a PhD degree from Nanyang Technological University, Singapore, respectively. Dr He is a Lecturer at Aston University, UK. His main research interests include mobile communications, 5G networks, connected vehicles, autonomous driving, Internet of things, AI for OCR and wireless newtorks. He has authored or co-authored over 100 technical papers in major international journals and conferences. He is an IEEE Senior Member.

Wenyang Guan received the B.Eng. degree in electronic information engineering from Jilin University, China, in 2005, and the M.S. and Ph.D degree in advanced telecommunication from Swansea University, Swansea, UK, in 2008 and 2013, respectively. From 2013 to 2015, he was a Postdoctoral Research Associate with Peking University. He is currently a lecturer in Beijing Technology and Business University. His research interests include MIMO systems, FPGA programming and wireless communications.

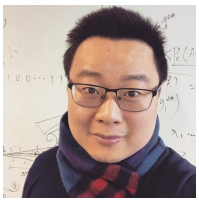

Dr. Weisi Guo (S07-M11-SM16) is an associate professor at the University of Warwick and a Turing Fellow at the Alan Turing Institute. His expertise is in signal processing and networks, and has been PI on over 2.4m of funding in a variety of communication and cyberphysical projects. He has published over 100 IEEE papers, won the IET Innovation Award, and been shortlisted for the Bell Labs Prize three times.

Wei Liu (M'06) received the B.S. degree in Telecommunication Engineering in 1999 and Ph.D. in Electronics and Information Engineering in 2004, both from Huazhong University of Science and Technology, Wuhan 430074, China. He is currently a professor with the School of Electronic Information and Communications, Huazhong University of Science and Technology. His research interests include network measurement, learning evalution, and etc.

Wenqing Cheng received the B.S. degree in Telecommunication Engineering in 1985 and Ph.D. in Electronics and Information Engineering in 2005, both from Huazhong University of Science and Technology, Wuhan 430074, China. She is currently a professor with the School of Electronic Information and Communications, Huazhong University of Science and Technology. Her research interests include communication systems, e-Learning applications, and etc.